Journal of Power Sources 230 (2013) 1–9

Contents lists available at SciVerse ScienceDirect

Journal of Power Sources

journal homepage: www.elsevier.com/locate/jpowsour

The effects of different oxidants on the characteristics of conductive polymer aluminum solid electrolyte capacitors

Myeongjin Kim, Jeeyoung Yoo, Hyungu Im, Jooheon Kim*

School of Chemical Engineering & Materials Science, Chung-Ang University, Seoul 156-756, Republic of Korea

HIGHLIGHTS

- ► Synthesized oxidant show high doping level and electrical conductivity.
- ► Higher doping level prevents the dielectric oxide films from damage.
- ► Decreased damaged surface area help to enhance the capacitance and leakage current.
- ► Enhanced electrical conductivity affect to the decrease of ESR property.
- ► Newly synthesized electrolytes exhibit excellent electrochemical performance.

ARTICLE INFO

Article history:
Received 23 October 2012
Received in revised form
7 December 2012
Accepted 8 December 2012
Available online 20 December 2012

Keywords:
Aluminum solid electrolyte capacitors
Conductive polymer
Poly(3,4-ethylenedioxythiophene
Doping level

ABSTRACT

Three kinds of oxidant are synthesized, ferric benzenesulfonate ($Fe(OBs)_3$), ferric 4-methylbenzenesulfonate ($Fe(OMBs)_3$), and ferric 4-ethylbenzenesulfonate ($Fe(OEBs)_3$). Then, 3,4- ethylenedioxythiophene (EDOT) is polymerized with these oxidants to obtain benzenesulfonate-doped poly(3,4- ethylenedioxythiophene) (PEDOT-OBs), 4-methyl-benzenesulfonate-doped poly(3,4- ethylenedioxythiophene) (PEDOT-OMBs) and 4-ethyl-benzenesulfonate-doped poly(3,4- ethylenedioxythiophene) (PEDOT-OEBs), respectively. PEDOT-OBs had the highest surface conductivity among the fabricated materials, because PEDOT-OBs had a better defined crystalline structure than the other polymers and the doping concentration of PEDOT-OBs is much higher than that of PEDOT-OMBs and PEDOT-OEBs. The capacitance of PEDOT-OBs is higher than those of PEDOT-OMBs and PEDOT-OEBs while the equivalent series resistance (ESR) and leakage current values of PEDOT-OMBs is lower than those of PEDOT-OMBs and PEDOT-OEBs because of the high electrical conductivity and low amount of undoped oxidant in PEDOT-OBs. Thermal degradation of all polymerized materials occur in the range of 300–330 °C, indicating that all of the polymerized materials had excellent thermal stability.

1. Introduction

Aluminum solid electrolyte capacitors based on conductive polymers have attracted considerable attention because of their extremely low impedance at high frequencies and reliability [1–7]. These types of capacitors are used in high-performance digital equipment such as liquid crystal displays, personal computers, and other electronic devices. Further improvement of these devices requires higher capacitor performance.

The most widely used conductive polymer is poly(3,4-ethylenedioxythiophene)-poly(styrenesulfonate) (PEDOT-PSS) [8]. PEDOT-PSS, however, has an electrical conductivity of only $\sim 10\ Scm^{-1}$, and therefore does not meet the requirements for high capacitance in aluminum solid electrolyte capacitors [9]. To generate polymers with high electrical conductivity and performance when used in aluminum solid electrolyte capacitors, ferric 4-methyl-benzenesulfonate ($Fe(OMBs)_3$) has been used as both an initiator and oxidizing agent. Pettersson used $Fe(OMBs)_3$ during the polymerization process to achieve high electrical conductivity (up to $550\ Scm^{-1}$) [10], and Kim reported the effect of organic solvents when $Fe(OMBs)_3$ was used instead of poly(styrenesulfonate) (PSS) [11].

Although aluminum solid electrolyte capacitors with 4-methyl-benzenesulfonate-doped poly(3,4- ethylenedioxythiophene) (PEDOT-OMBs) shows superior performance to PEDOT-PSS, their capacitance could be improved, and their equivalent series resistance (ESR) and leakage current decreased. One reason for the non-optimal performance of PEDOT-OMBs capacitors is damage to the boundary of the dielectric layer. Low doping between

* Corresponding author. Tel.: +82 2 820 5763; fax: +82 2 812 3495.
E-mail address: jooheonkim@cau.ac.kr (J. Kim).

0378-7753/$ – see front matter © 2012 Elsevier B.V. All rights reserved.
http://dx.doi.org/10.1016/j.jpowsour.2012.12.038

PEDOT and $Fe(OMBs)_3$ corresponds to high levels of undoped oxidant. This can strongly affect the extent of damage to the boundary between PEDOT-OMBs and the dielectric layer, because residual oxidants can react with hydroxyl groups and/or absorbed water on the aluminum oxide surface [12]. Yamamoto and colleagues reported that because the dielectric layer of an electrolyte capacitor is formed by anodic oxidation of valve metals, a dielectric layer consisting of aluminum oxide has a rectifying action. Therefore, capacitor performance is degraded by deoxidizing reactions between the dielectric metal oxide layer and electrolyte [13].

Nogami suggested a new type of dielectric layer coated with hyperbranched poly(siloxysilane)s (HBPSi) that have a large number of vinyl groups to improve the interfacial interaction between aluminum oxide and PEDOT. Capacitors coated with HBPSi on the dielectric layer showed enhanced capacitance and lower ESR and leakage current, because HBPSi helped inhibit the undoped oxidant-induced degradation of the dielectric oxide layer [12].

Efforts to improve the oxidant properties, such as ionic conductivity and degree of dissociation, of aluminum solid electrolyte capacitors in order to reduce damage to the surface area of the boundary between the dielectric oxide layer and the electrolyte have only recently been reported. In this study, a new type of oxidant, ferric benzenesulfonate ($Fe(OBs)_3$), was developed for enhanced doping level to prevent damage to the boundary layer between PEDOT-OBs and the dielectric layer in aluminum solid electrolyte capacitors. Ferric 4-ethylbenzenesulfonate ($Fe(OEBs)_3$) was also developed to compare the effects of substituted alkyl groups. Before application to aluminum solid electrolyte capacitors, benzenesulfonate-doped poly(3,4- ethylenedioxythiophene) (PEDOT-OBs), PEDOT-OMBs, and 4-ethyl-benzenesulfonate-doped poly(3,4- ethylenedioxythiophene) (PEDOT-OEBs) were chemically polymerized from their monomers and oxidants, and their conducting behavior in terms of surface conductivity, doping level, ionic conductivity, and structure properties were investigated. Aluminum solid electrolyte capacitors were prepared using a counter electrode and PEDOT-OBs, PEDOT-OMBs, or PEDOT-OEBs as electrolyte materials, respectively, to determine the effects of the polymerized materials on a variety of electrochemical properties of the resulting capacitors, including their capacitance, ESR, and leakage current.

2. Experimental

2.1. Synthesis of $Fe(OBs)_3$, $Fe(OMBs)_3$, and $Fe(OEBs)_3$

The overall reaction mechanism is illustrated in Fig. 1. To synthesize 4-alkyl-benzenesulfonic acid, alkylbenzene was reacted with sulfonic acid at 150 °C for 1 h. The mole ratio between alkylbenzene and sulfonic acid was 1:1. After the reaction, products were obtained by recrystallization of alkylbenzene using a rotary evaporator. The obtained 4-alkyl-benzenesulfonic acid was dried in a vacuum oven at 60 °C for 1 h. Finally, to obtain $Fe(OBs)_3$, $Fe(OMBs)_3$, and $Fe(OEBs)_3$, the 4-alkyl-benzenesulfonic acid was dispersed in methanol, and ferric chloride hexahydrate ($FeCl_3 \cdot 6H_2O$) was added to the mixture dropwise at 230 °C for 1 h. The mole ratio between ferric chloride hexahydrate and 4-alkyl-benzenesulfonic acid was 1:3. The resulting powder was filtered and refluxed for 30 min in methanol/acetonitrile solvent. The resulting product was then filtered and dried in a vacuum oven at 60 °C for 30 min.

2.2. Polymerization

PEDOT-OBs was polymerized chemically from prepared EDOT (Baytron M, Bayer) and ferric benzenesulfonate ($Fe(OBs)_3$). In the polymerization reactions, EDOT was used as a monomer and $Fe(OBs)_3$ was used as both an initiator and oxidizing agent. Before starting polymerization, $Fe(OBs)_3$ was dried in a vacuum oven at 80 °C for 48 h. Then, $Fe(OBs)_3$ was dispersed in methanol for 1 h. After that, EDOT was added to the mixture to create polymer chains. The mole ratios of the monomers and the oxidant were 1:0.6, 0.8, 1.0, 1.2, 1.4, 1.6, 1.8, 2.0, and 2.2, respectively. The temperature of the reaction was maintained at 40 °C for 30 min with vigorous stirring. The temperature was then increased to 180 °C, and stirring was sustained for 20 min to terminate the polymerization reaction. The product was filtered with a nylon filter and washed with methanol several times to remove residual monomers of $Fe(OBs)_3$, and dried in a vacuum oven at 80 °C for 24 h. PEDOT-OMBs and PEDOT-OEBs were polymerized in the same manner as described for PEDOT-OBs.

2.3. Fabrication of Al solid electrolyte capacitors

Aluminum solid electrolyte capacitors with PEDOT-OBs as the electrolyte were fabricated as follows. Electrochemically-etched aluminum foil (2.5 mm × 140 mm × 0.1 mm) was anodized at 4 V to form an aluminum oxide dielectric layer. The aluminum foil and acryl fabric separators were wound together to form an element. The surface of the aluminum oxide film on the aluminum foil was coated with the doped PEDOT-OBs by dipping the film in an ethanol solution of $Fe(OBs)_3$ containing EDOT, followed by heating at 180 °C to induce polymerization. The element was sealed in an aluminum can identical to that used for electrolytic aluminum capacitors. A 3 V DC current was then applied for 1 h at 130 °C to

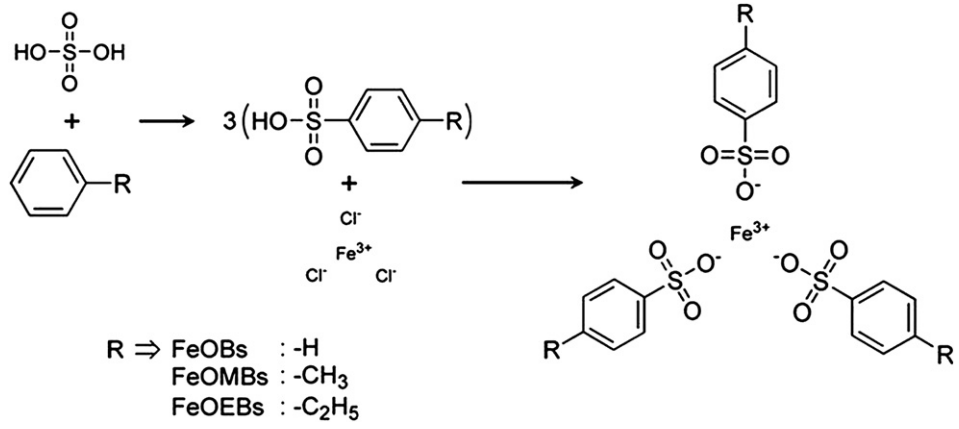

Fig. 1. Chemical routes for the synthesis of $Fe(OBs)_3$, $Fe(OMBs)_3$, and $Fe(OEBs)_3$.

reduce the leakage current. A schematic view of the fabricated device is provided in Fig. 2. Capacitors with PEDOT-OMBs and PEDOT-OEBs were fabricated as described above for capacitors with PEDOT-OBs.

2.4. Characterization methods

Nuclear magnetic resonance spectroscopy (600 MHz, VNS/Varian) was used to characterize the chemical structure of the resultant oxidants. D_2O was used as a solvent. For the FT-IR measurements, the synthesized materials were pressed into pellets with potassium bromide (KBr) and scanned using radiation ranging in frequency from 400 to 4000 cm^{-1}. The surface conductivity the PEDOT-OBs, PEDOT-OMBs, and PEDOT-OEBs was measured using a four-probe method. The doping level between the monomers and oxidant was investigated by X-ray photoelectron spectroscopy (XPS, VGMicrotech, ESCA2000) using a spectrometer with an Mg Ka X-ray source (1253.6 eV) and a hemispherical analyzer. During curve fitting, the Gaussian peak widths were constant in each spectrum. The ionic conductivity of $Fe(OBs)_3$, $Fe(OMBs)_3$, and $Fe(OEBs)_3$ in solvent (ethanol) was measured with an electrochemical conductivity meter (TOA, CM-6092). The orthorhombic structure of PEDOT-OBs, PEDOT-OMBs, and PEDOT-OEBs was characterized using an X-ray diffractometer (XRD, New D8-Advance/Bruker-AXS) at a scan rate of 1° s^{-1} with a 2θ range of 5–35° with $CuK_{\alpha 1}$ radiation (0.154056 nm). The capacitance and equivalent series resistance (ESR) from 1 Hz to 1 MHz were measured with a frequency response analyzer (IM6, Zahner). The leakage current (LC) was measured with a multimeter (HP34401A, Agilent) and DC power supply (HP6654A, Agilent). Thermogravimetric analysis (TGA, TGA-2050, TA instrument) of the samples was carried out to examine the thermal degradation of PEDOT-OBs, PEDOT-OMBs, and PEDOT-OEBs. Samples (5 mg) were heated to 80 °C and kept at this temperature to remove water. These samples were reheated to 600 °C at a heating rate of 10 °C min^{-1} under a nitrogen atmosphere.

3. Result and discussion

3.1. Structure analysis

Chemical structures of the synthesized oxidants were determined using NMR spectroscopy and FT-IR, and the analyzed NMR results are shown in Fig. 3(a)–(c). There were solvent (D_2O) peak at 4.9 ppm in the all NMR spectra. As shown in Fig. 3(a), $Fe(OBs)_3$ has characteristic peaks corresponding to the two kinds of proton resonance. The peak at 7.4 ppm represents the proton arising from the meta-position of benzenesulfonate. The peak at 7.7 ppm originates from proton on the ortho-position of benzenesulfonate. The ^1H NMR spectrum of $Fe(OMBs)_3$ is provided in Fig. 3(b). The peaks

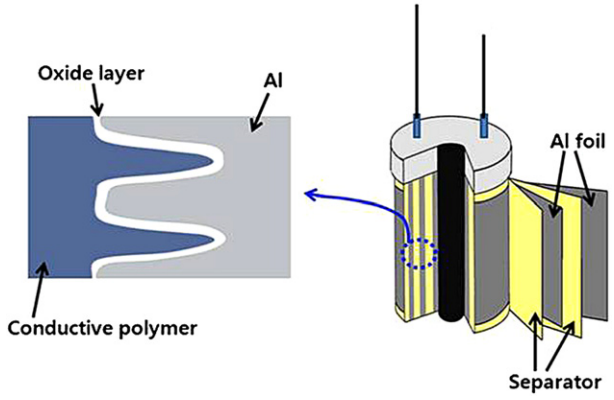

Fig. 2. A schematic of an aluminum solid electrolyte capacitor (wound type). Conductive polymer: PEDOT-OBs, PEDOT-OMBs, or PEDOT-OEBs.

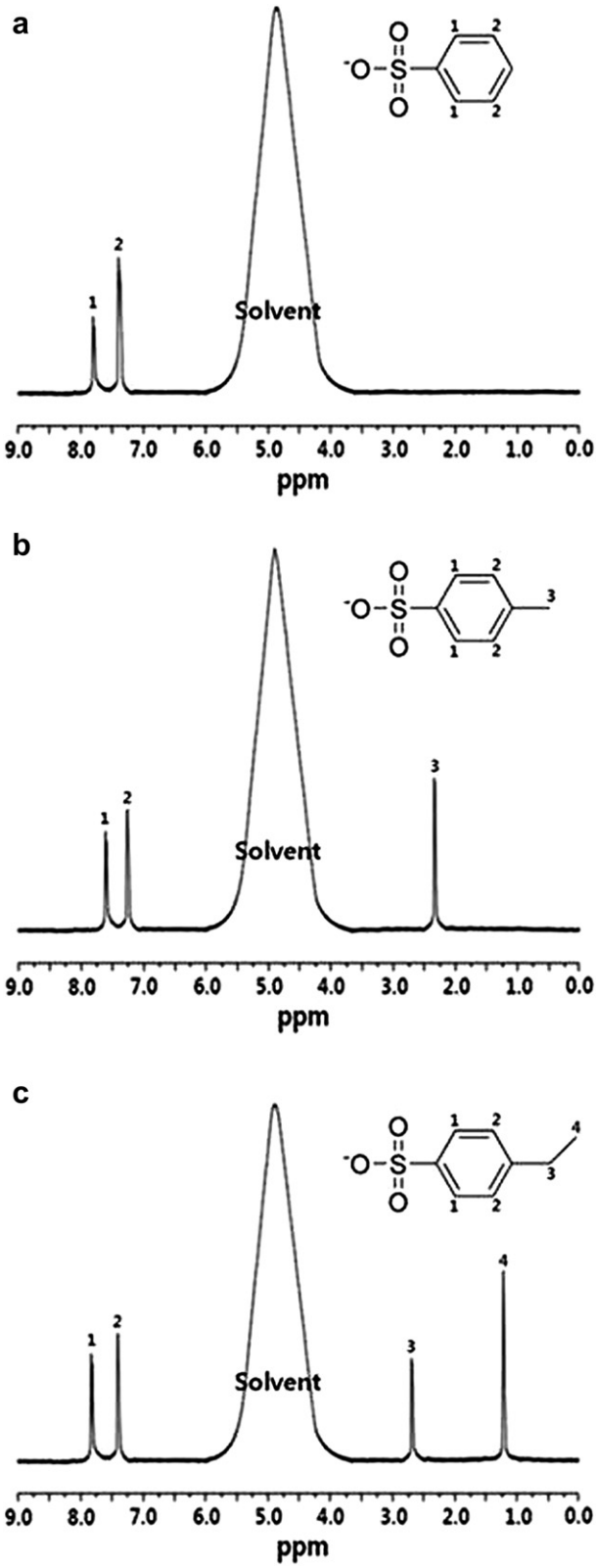

Fig. 3. ^1H NMR spectrum of (a) $Fe(OBs)_3$, (b) $Fe(OMBs)_3$, and (c) $Fe(OEBs)_3$.

at 7.3 and 7.6 ppm are attributed to the resonance of the meta- and ortho- positions of methylbenzenesulfonate, respectively. The resonance peak at 2.3 ppm is ascribed to the proton of the methyl group on the para-position of methylbenzenesulfonate. In Fig. 3(c), characteristic peaks of $Fe(OEBs)_3$ corresponding to four kinds of proton resonance are evident. The peaks at 7.4 and 7.7 ppm were assigned to the resonance of the meta- and ortho-positions of ethylbenzenesulfonate, respectively. The resonance peaks at 2.6 and 1.2 ppm were assigned to the proton of the ethyl group on the para-position of ethylbenzenesulfonate. The peak at 2.6 ppm is attributed to the resonance of the methyl group substituted on the para-position of benzenesulfonate, and the peak at 1.2 ppm is ascribed to the proton of the rest of the methyl group, which is linked to the methyl group substituted on the para-position of benzenesulfonate [14].

FT-IR was used to characterize the synthesis of the oxidants. Fig. 4(a)–(c) shows the FT-IR spectra of $Fe(OBs)_3$, $Fe(OMBs)_3$, and $Fe(OEBs)_3$, respectively. For $Fe(OBs)_3$, the bands at 1450–1600 cm^{-1}, 944–1341 cm^{-1}, and 513–791 cm^{-1} represent the stretching of the benzene ring, S=O, and S–C in all the oxidants, respectively. In addition, the new band at the high frequency of 2950–2975 cm^{-1} corresponds to stretching of the methyl group ($-CH_3$) in $Fe(OMBs)_3$ (Fig. 4(b)). In $Fe(OEBs)_3$ (Fig. 4(c)), the presence of a band at 2960–3000 cm^{-1} reflects stretching of the ethyl group ($-C_2H_5$) [15]. These results indicate that $Fe(OBs)_3$, $Fe(OMBs)_3$, and $Fe(OEBs)_3$ with the desired molecular structure were synthesized.

3.2. Conducting behavior of polymerized EDOT materials

It is well known that the conducting behavior of conductive polymer electrolytes has a significant impact on capacitor properties such as impedance, equivalent series resistance (ESR), and dielectric loss factor (tan δ). In particular, the equivalent series resistance (ESR) is directly affected by the resistance of the conductive polymer electrolyte, because a conductive polymer electrolyte with high resistance can significantly increase the ESR. For real-world applications, aluminum solid electrolyte capacitors should have a high capacitance and a low ESR. To ensure that the ESR of the capacitor was low, it was optimized that the oxidant content of the conducting polymer to maximize electrical conductivity.

The surface conductivity of the three kinds of polymerized EDOT is investigated as a function of oxidant content, and the results are shown in Fig. 5. The maximal electrical surface conductivity is observed at a 0.8 molar ratio in equivalent monomers, regardless of the identity of the oxidant. The electrical conductivity decrease dramatically as the quantity of oxidant increased.

The reason for this result is the increase in concentration of undoped oxidant in the polymer chain. The oxidants were ionized to cations (Fe^{3+}) or anions (OBs^-, $OMBs^-$, and $OEBs^-$) during the polymerization process. Then, the OBs^-, $OMBs^-$, and $OEBs^-$ ions were doped on the polymer chain, conferring them with conductive properties. However, when greater than 0.8 mol of oxidant is added, two types of oxidants were present in the polymerized material: OBs^-, $OMBs^-$ and $OEBs^-$ doped on the polymer chain, and $Fe(OBs)_3$, $Fe(OMBs)_3$, and $Fe(OEBs)_3$ undoped on the polymer chain in an unionized state. These residual undoped oxidants in the polymer function as resistance components [16].

Note that the oxidant content in the conducting polymer provides the maximal electrical conductivity when held at the constant mole ratio of 0.8. Moreover, the surface conductivity of PEDOT-OBs is the highest among the polymerized materials, regardless of oxidant content. This result is correlated to the oxidant doping ratio in the polymerized chain [11]. To analyze the oxidant doping ratio, XPS analysis was performed and the S 2p core-level spectra for the polymerized materials and oxidants are shown in Fig. 6.

Because of different chemical environments, the S 2p electrons of PEDOT-OBs, PEDOT-OMBs, PEDOT-OEBs, and the oxidants have different binding energies. In Fig. 6(a)–(c), the lower binding energy peaks at 163.9 and 165 eV correspond to the spin-split doubles of the sulfur atoms in PEDOT. The higher binding energy peak at 169.1 eV corresponds to the sulfur atom in alkylbenzenesulfonate ions. Comparison of the spectrum of oxidants enables

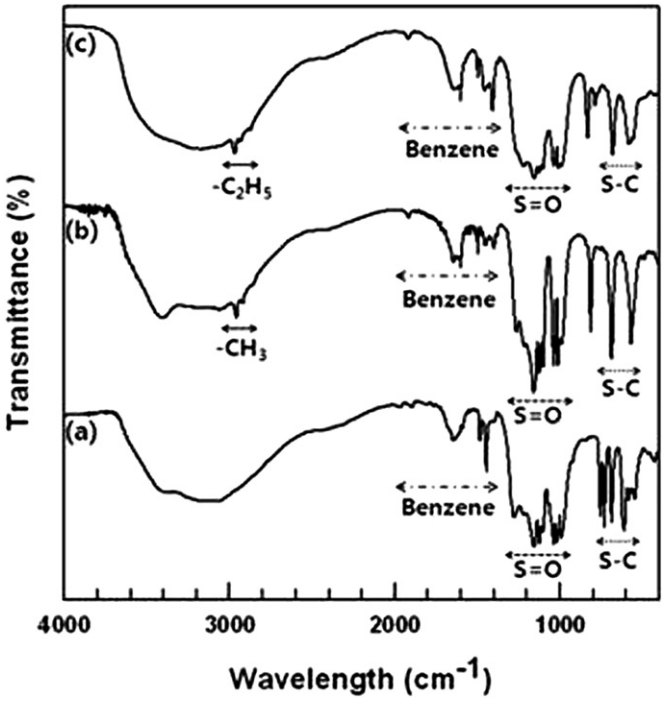

Fig. 4. FT-IR spectrum of (a) $Fe(OBs)_3$, (b) $Fe(OMBs)_3$, and (c) $Fe(OEBs)_3$.

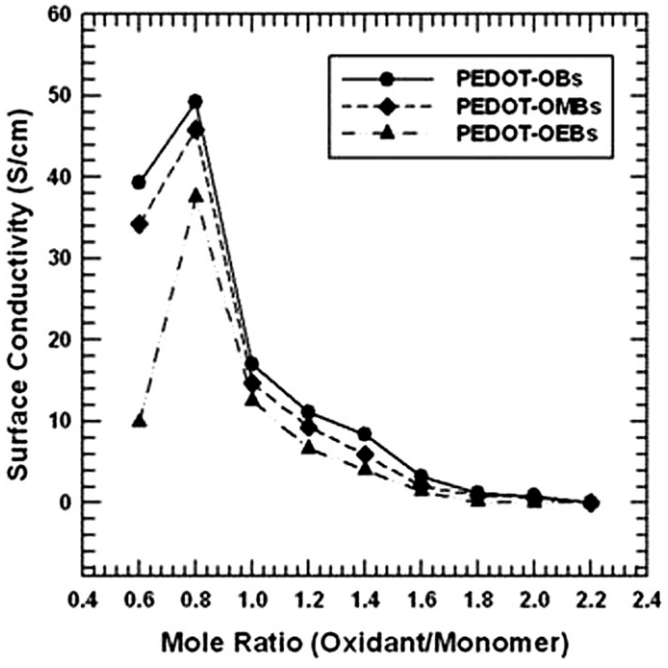

Fig. 5. Surface conductivity of PEDOT-OBs, PEDOT-OMBs, and PEDOT-OEBs.

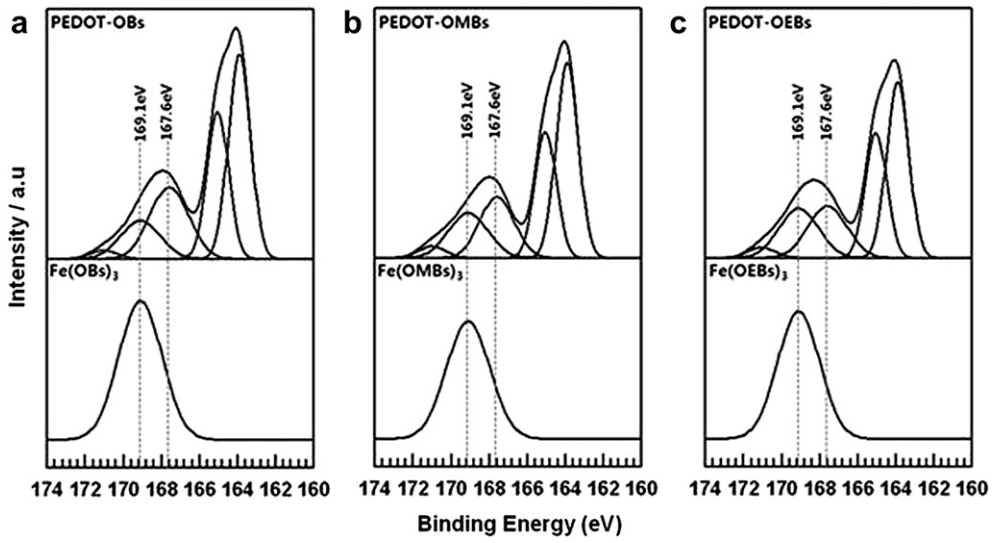

Fig. 6. XPS spectra of the S 2p core level of (a) PEDOT-OBs and $Fe(OBs)_3$, (b) PEDOT-OMBs and $Fe(OMBs)_3$, and (c) PEDOT-OEBs and $Fe(OEBs)_3$.

deconvolution of the S 2p signal associated with alkylbenzenesulfonate ions into two types of spin-split doubles. The S $2p_{3/2}$ peak located at 169.1 eV originates from the sulfonic acid group of the oxidants, while the additional S $2p_{3/2}$ peak at 167.6 eV originates from the sulfonate group, $PEDOT^{+}SO_3^{-}$, consistent with previously reported data [9]. Based on these results, it can be concluded that successful doping of PEDOT-OBs, PEDOT-OMBs, and PEDOT-OEBs with oxidants results in the formation of free radicals in the polymer chain and contributes to the conducting behavior of EDOT. The ratio of $PEDOT^{+}SO_3^{-}$ to the PEDOT signal allows direct estimation of the doping level [11]. Based on the measured area ratio, it is observed that PEDOT-OBs have a molecular doping level of 34.9 at.%, higher than that of PEDOT-OMBs (31.5 at.%) and PEDOT-OEBs (29.3 at.%). This result implies that the presence of substituted alkyl groups in the oxidant decreases the oxidant doping level and lead to a slight decrease in surface conductivity compared with that of PEDOT-OBs, as illustrated in Fig. 6.

Differences in surface conductivity and doping level were correlated with the ionic conductivity of the three kinds of oxidants. In Fig. 7, it can be seen that the ionic conductivity of $Fe(OBs)_3$ is the highest among the oxidants, regardless of oxidant concentration. This result implies that in the case of $Fe(OBs)_3$, a high level of ion dissociation is achieved and that a large amount of mobile ions were produced. The relatively higher doping level of PEDOT-OBs relative to the other polymers can be explained by the greater availability of mobile ions when $Fe(OBs)_3$ is used as the oxidant, because more ions were available to participate in the doping process [11].

When an oxidant is dissolved in a solvent, ion dissociation occurs through the process of solvation, leading to ionic conductivity. If the oxidants are completely dissociated, nearly all of the cations (Fe^{3+}) or anions (OBs^{-}, $OMBs^{-}$ and $OEBs^{-}$) are available for doping. However, if the oxidants are not completely dissociated, then there is a decrease in the concentration of ions, which will lower ionic conductivity. The ionic bond between cations and anions must be broken for dissociation in a solvent. The bond strength between cations and anions therefore has a large effect on the dissociation process. $Fe(OMBs)_3$ and $Fe(OEBs)_3$ contain alkyl groups ($-CH_3$ and $-C_2H_5$) that have a tendency to donate electrons when linked to some other group or part of some other molecule [17]. Furthermore, sulfonated ($-SO_3^{-}$) is an electron-withdrawing group when attached to a benzene molecule, and decreases the electron density of the benzene ring. These alkyl groups, which are linked to the para- position of benzene sulfonate, release electron density to the neighboring benzene, and also to the sulfonate bonded with Fe^{3+}. The release of electron density to sulfonate creates a partial negative charge on the sulfonate group. Considering the alkyl groups substituted on the para-position, the sulfonate group of $Fe(OEBs)_3$ substituted for the ethyl groups showed the highest concentration of partial negative charge compared to the other two oxidants ($Fe(OBs)_3$ and $Fe(OMBs)_3$), because ethyl groups provide more electrons that can be donated than methyl groups. As expected, the rank order of partial negative charge on the sulfonate group of the oxidants is $Fe(OEBs)_3 > Fe(OMBs)_3 > Fe(OBs)_3$. This means that the ionic bond strength

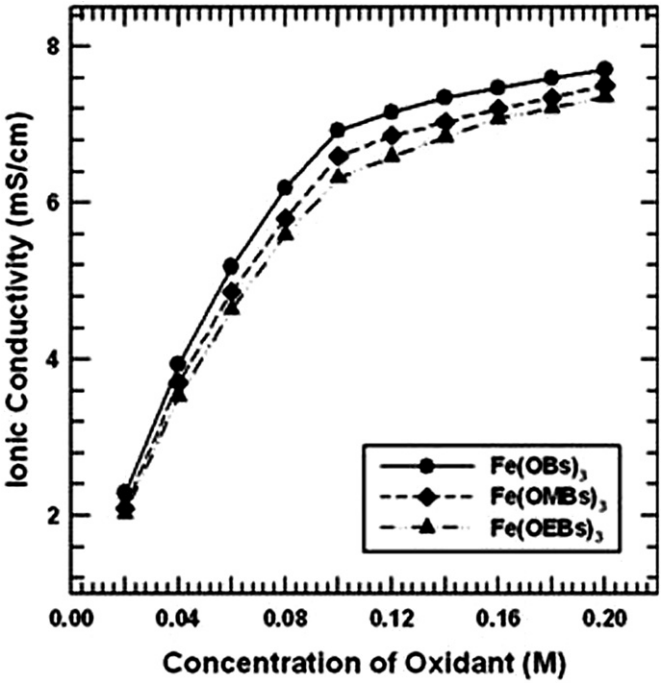

Fig. 7. Ionic conductivity of $Fe(OBs)_3$, $Fe(OMBs)_3$, and $Fe(OEBs)_3$.

between the sulfonate group and Fe^{3+} is different in the different oxidants because of differences in partial electron concentrations among the oxidants. The oxidants should have the same order of ionic bond strength as the rank order of partial negative charge on the sulfonate group. The ionic conductivity of $Fe(OBs)_3$ is the highest, because it has the highest level of ion dissociation among the three oxidants evaluated due to its weak ionic bond strength and partial negative charge tendency. A stronger ionic bond between the cations and anions reduces the level of dissociation, thereby decreasing the amount of mobile ions that can participate in the doping process, which leads to a decrease in the doping level and conductivity.

The change in the chain structure of the oxidants induced by the substituted alkyl groups provides an explanation for the different conductivities of PEDOT-OBs, PEDOT-OMBs and PEDOT-OEBs. X-ray diffraction patterns of PEDOT polymerized with different oxidants are shown in Fig. 8. Characteristic diffraction peaks of PEDOT-OBs, PEDOT-OMBs, and PEDOT-OEBs are visible, indicating the existence of a crystalline phase. Similar to previous XRD analysis of PEDOT-OMBs with an orthorhombic structure, PEDOT-OMBs (Fig. 8(b)) has diffraction peaks at $2\theta = 6.2^\circ$, 12.2°, and 25.8° that could be assigned to (1 0 0), (2 0 0), and (0 2 0) reflections, with lattice parameters of $a = 14.3$ Å, $b = 6.8$ Å, and $c = 7.8$ Å, respectively. The repeat unit of the PEDOT-OMBs chain is determined by the unit cell constant, c. It is assumed to be 7.8 Å according to the previously reported value. The PEDOT-OMBs chains stack on top of each other with a stacking distance of $b/2 = 3.4$ Å and the bc-layers were separated by counter ions along the a-axis [18,19].

As shown in Fig. 8(a), the diffraction peaks of PEDOT-OBs at 2θ scattering angles of $\sim 6.8^\circ$, 13°, and 26.2° were assigned to (1 0 0), (2 0 0), and (0 2 0) reflections. PEDOT-OBs shows more pronounced diffraction peaks than PEDOT-OMBs and PEDOT-OEBs, and the peak positions corresponding to the (1 0 0), (2 0 0), and (0 2 0) reflection planes were shifted to slightly higher angles than those of PEDOT-OMBs and PEDOT-OEBs. The conductivity of PEDOT is strongly affected by the stacking distance along the b-axis, the conjugated polymer backbone along the c-axis, and the interchain distance within the stack along the a-axis due to orbital overlap. In the case of PEDOT-OBs, because the unit cell constant b or $b/2$ describes the distance between the chains stacking on top of each other, the shift of the (0 2 0) peak position to a higher angle indicates a decrease in the stacking distance. Furthermore, the shift of the (2 0 0) reflection plane to a higher angle corresponds to a short distance between neighboring thiophene rings in the conjugated polymer backbone. In addition, the PEDOT-OBs chain is short and well defined within the co-facial stack, because the (1 0 0) peak position is thought to be related to the interchain distance within the stack.

Therefore, substitution of shorter alkyl groups, such as $Fe(OBs)_3$, on para-positions of PEDOT during polymerization results in improved packing of the PEDOT chains, resulting in increased charge carrier hopping between the chain stacks and carrier hopping within the stack. In contrast, the introduction of longer alkyl groups, such as $Fe(OEBs)_3$, reduces the overall conductivity of the PEDOT chains, either by increasing the separation of the co-facial stacks or chains within the stack.

3.3. Electrochemical behavior

The electrode interface of the conductive polymer on an aluminum oxide layer is simulated, and the results are shown in Fig. 9. The frequency dependence of capacitance in capacitors fabricated using doped PEDOT-OBs, PEDOT-OMBs, and PEDOT-OEBs is shown in Fig. 10. In particular, because capacitors in electronic devices have to operate at high-frequency ranges (i.e. over 1 kHz), capacitance behavior beyond 1 kHz is regarded a critical characteristic of capacitors [20]. The capacitances of the various capacitors show similar behavior regardless of chemical structure. As expected, the capacitance values of the capacitors decrease in the order PEDOT-OBs > PEDOT-OMBs > PEDOT-OEBs over the entire frequency range, as shown in Fig. 10. The equation that relates capacitance and other factors is as follows:

$$C = \varepsilon \frac{S}{d} \tag{1}$$

where ε, S, and d are the dielectric constant of the dielectric, surface area of the dielectric, and the thickness of the dielectric oxide film on etched aluminum foil, respectively [21]. In this experiment, the surface area of the dielectric, which is proportional to capacitance, is the most important parameter, because the dielectric constant and the thickness of the dielectric are fixed. In addition, the surface area of the dielectric corresponding to the contact area between the electrolyte and the dielectric layer on the electrode strongly affects the extent of damage to the boundary between the electrolyte and the dielectric layer caused by undoped oxidant. Residual oxidants were present in the capacitors, because unreacted oxidants were not removed when the conductive polymers were applied to the aluminum solid electrolyte capacitors. These undoped oxidants

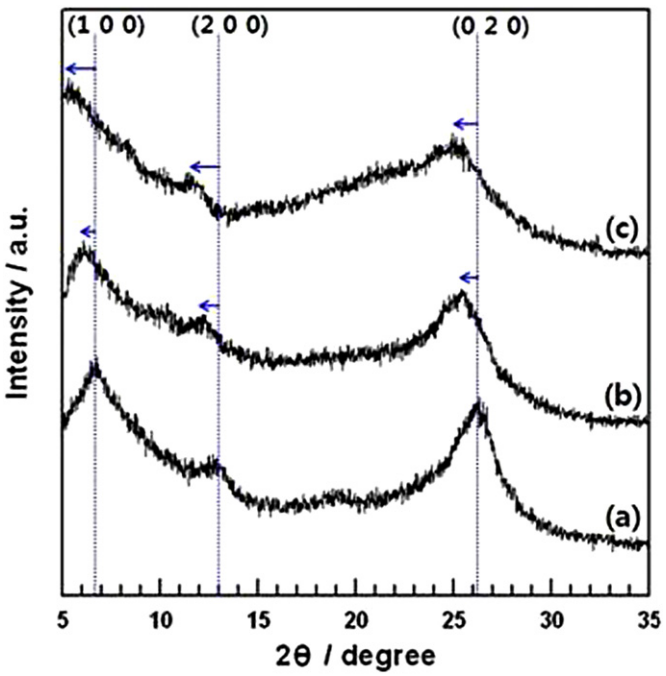

Fig. 8. XRD patterns of (a) PEDOT-OBs, (b) PEDOT-OMBs, and (c) PEDOT-OEBs.

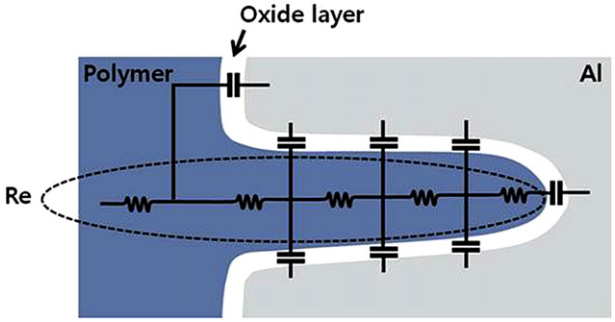

Fig. 9. The equivalent circuit for a capacitor with an etched aluminum surface.

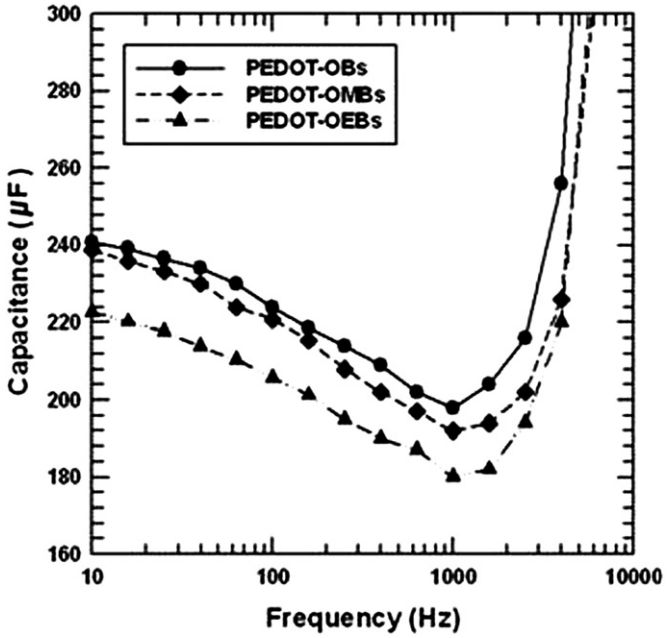

Fig. 10. Capacitance–frequency characteristics of capacitors synthesized using PEDOT-OBs, PEDOT-OMBs, and PEDOT-OEBs.

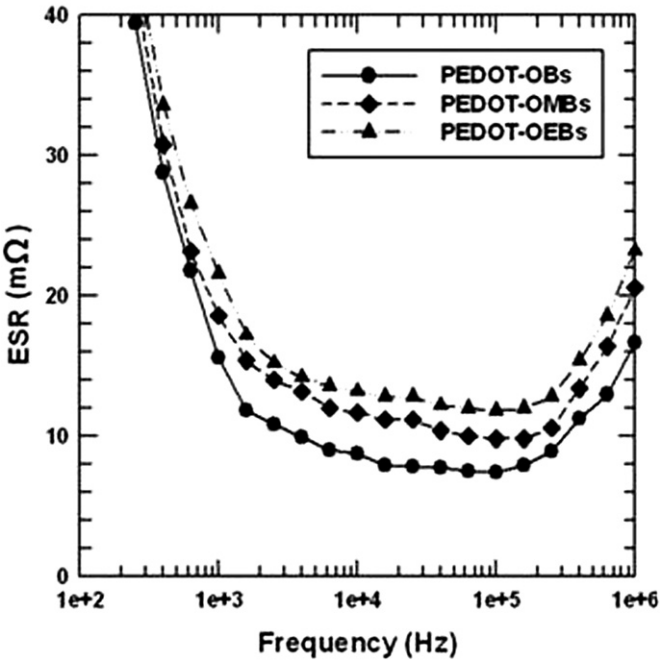

Fig. 11. Equivalent series resistance-frequency characteristics of the capacitors synthesized using PEDOT-OBs, PEDOT-OMBs, or PEDOT-OEBs.

could potentially have reacted with hydroxyl groups and/or absorbed water on the dielectric layer (aluminum oxide surface), resulting in the formation of $Fe(OH)_3$, alkylbenzenesulfonic acid. Alkylbenzenesulfonic acid can cause defects and surface dissolution of the dielectric layer [12,13]. In previous XPS analyses, the S $2p_{3/2}$ peak located at 169.1 eV is assigned to the alkylbenzenesulfonic acid group of the oxidants. Based on these results, it can be concluded that undoped oxidants in the PEDOT chain formed alkylbenzenesulfonic acid. In Fig. 5, Polymerized PEDOT materials listed in order of doping level are PEDOT-OBs > PEDOT-OMBs > PEDOT-OEBs. This can be explained by the higher doping level providing lower concentration of undoped oxidant. Therefore, the order of concentration of alkylbenzenesulfonic acid in the PEDOT polymers is PEDOT-OEBs > PEDOT-OMBs > PEDOT-OBs. This indicates that the extent of damaged surface area of the dielectric layer is PEDOT-OEBs > PEDOT-OMBs > PEDOT-OBs. The PEDOT-OBs shows the highest capacitance value over the whole range of frequencies because PEDOT-OBs has the least damaged dielectric surface layer. The capacitance behaviors of PEDOT-OBs, PEDOT-OMBs, and PEDOT-OEBs were consistent with the extent of damaged surface area and the concentration of alkylbenzenesulfonic acid in each PEDOT polymer type. It is believed that the higher doping level was able to increase the capacitance of aluminum solid electrolyte capacitors due to preventing the dielectric oxide films from damage which are contributing to increasing the contact area because of improved adhesion of the interface between the dielectric oxide film and the PEDOT.

The measured ESR values of capacitors fabricated in this study are shown in Fig. 11. Generally, because capacitors are used in high-frequency applications, a lower ESR is required at a higher frequency [20]. The Rs for the equivalent circuits of the capacitors were expressed using the following equation:

$$\mathrm{Rs} = \frac{\tan\delta}{2\pi f C} + \mathrm{Re} \tag{2}$$

where tan δ, C, and Re are the dissipation factor of the dielectric oxide film, capacitance at the frequency f, and resistance due to the conductive polymer of the etching pits, respectively. The ESR values of the capacitors are shown in Fig. 11. In general, resistance is inversely proportional to contact area, which is proportional to capacitance, as described previously. In polymer capacitors, the doping rate should also be considered, because the electrical conductivity of a polymer is directly related to its resistance. Therefore, Rs should be inversely proportional to capacitance and proportional to the doping rate of the polymer. Furthermore, unreacted oxidants and side product formed by reaction with the dielectric oxide layer ($Fe(OH)_3$, BSA, MBSA, EBSA) increase resistance. An improvement in Rs can be attributed to an increase in contact area between the dielectric layer and the polymer, and/or the doping rate of the polymer. As mentioned above, PEDOT-OBs had the largest contact area and showed the highest doping rate (PEDOT-OBs > PEDOT-OMBs > PEDOT-OEBs). This result is consistent with the capacitance behavior result.

To study leakage current characteristics, the leakage current (I) of the capacitors is measured when charged with positive and negative potentials (V). The V–I curves of PEDOT-OBs, PEDOT-OMBs, and PEDOT-OEBs capacitors are shown in Fig. 12. The PEDOT-OBs capacitor has the lowest leakage current over the whole voltage range of the different capacitors evaluated. The major reason for current leakage is the rectifying action of the dielectric oxide layer, because the dielectric of an electrolytic capacitor formed by anodic oxidation of valve metals can react with side products of the electrolyte during the polymerization process [13]. These results suggest that deoxidizing reactions of the dielectric oxide layer occurred readily in the PEDOT-OMBs and PEDOT-OEBs electrolytes, but not in the PEDOT-OBs electrolyte. This is also correlated to the oxidant doping ratio in the polymerized chain. The PEDOT-OEBs capacitor has more damaged surface area than the PEDOT-OBs and PEDOT-OMBs capacitors, causing the leakage current to increase because the concentration of undoped oxidant decreases in the order of PEDOT-OEBs > PEDOT-OMBs > PEDOT-OBs. Therefore, a high doping level can prevent damage to the dielectric oxide layer and decrease the leakage current of a capacitor.

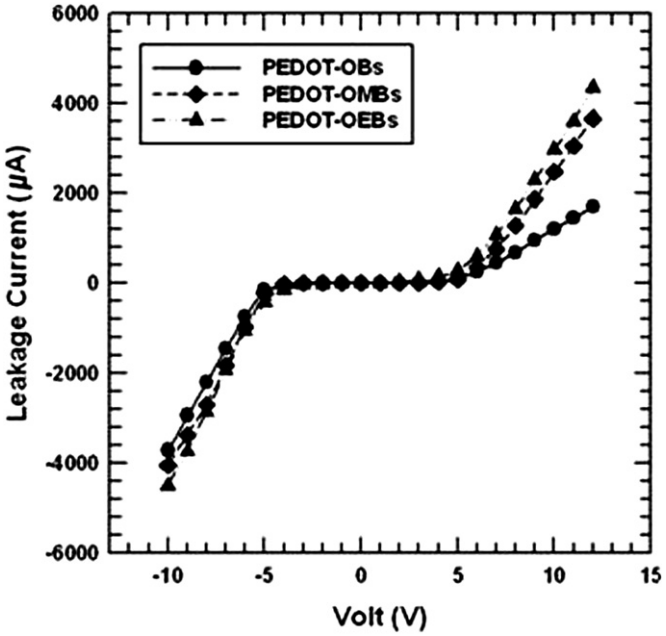

Fig. 12. Leakage current–voltage characteristics of the capacitors synthesized using PEDOT-OBs, PEDOT-OMBs, or PEDOT-OEBs.

In summary, the concentration of undoped oxidant in a capacitor is significantly correlated to its performance. A high doping level is crucial for the performance of a capacitor, because it decreases the amount of damaged surface area of the dielectric, and thereby improves the capacitance, ESR, and leakage current of the capacitor.

3.4. Thermal stability

The thermal stability of a conductive polymer electrolyte is an important determinant of its durability during operation at high temperatures. The thermal stability of PEDOT-OBs, PEDOT-OMBs, and PEDOT-OEBs was examined by TGA analysis. A TGA thermal graph of the polymerized materials is shown in Fig. 13. Thermal degradation of PEDOT-OBs, PEDOT-OMBs, and PEDOT-OEBs is observed at approximately 300–330 °C, which was assigned to deposition of the polymer main chain. At 300 °C, weight loss of the polymerized materials is observed. Considering the maximum operating temperature (105 °C) of the aluminum solid electrolyte capacitor, the thermal degradation profiles of the PEDOT-OBs, PEDOT-OMBs, and PEDOT-OEBs are excellent.

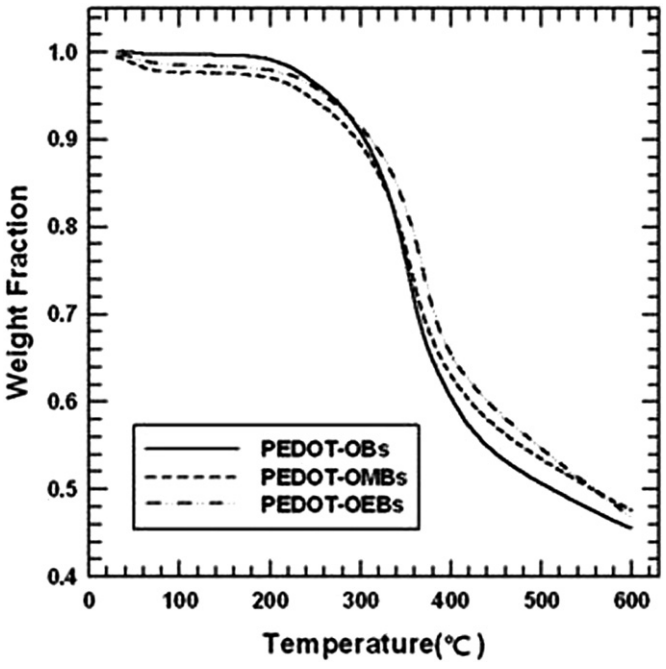

Fig. 13. Thermal analysis of the TGA curves for PEDOT-OBs, PEDOT-OMBs, and PEDOT-OEBs.

4. Conclusions

The three types of oxidants, $Fe(OBs)_3$, $Fe(OMBs)_3$, and $Fe(OEBs)_3$, were synthesized using alkylbenzene, sulfonic acid, and ferric chloride. Polymerized materials (PEDOT-OBs, PEDOT-OMBs and PEDOT-OEBs) were prepared using a chemical polymerization process between monomer (EDOT) and one of the three oxidants ($Fe(OBs)_3$, $Fe(OMBs)_3$ and $Fe(OEBs)_3$). The polymerized materials have maximum electrical surface conductivity at a molar ratio of 0.8 of equivalent monomer, regardless of the oxidant identity. Electrical conductivity decrease dramatically as the oxidant quantity increased. This may be attributed to the increase in concentration of undoped oxidant in the polymer chain as the quantity of oxidant increased to more than 0.8 mole. The residual undoped oxidant acts as a resistance component in the polymer. The surface conductivity of PEDOT-OBs is the highest among the polymerized materials, regardless of the oxidant content. This can be explained by the oxidant doping ratio in the polymerized chain. The molecular doping level of PEDOT-OBs (34.9 at.%) was much higher than that of PEDOT-OMBs (31.5 at.%) and PEDOT-OEBs (29.3 at.%). This result implies that a high level of ion dissociation is achieved in PEDOT-OBs, and that a larger amount of mobile ions were produced when $Fe(OBs)_3$ is used as the oxidant. Furthermore, X-ray diffraction patterns revealed that PEDOT-OBs have a more conductive structure with a shorter interchain and stacking distance than PEDOT-OMBs and PEDOT-OEBs. The increase in crystallinity of the conducting polymers does not introduce conjugation defects into the system, making the system more conductive. These superior conductive properties of PEDOT-OBs are attributed to capacitance, ESR and leakage current in the aluminum solid electrolyte capacitor. The capacitor containing PEDOT-OBs have higher capacitance and lower ESR value over the whole frequency range, and lower leakage current value over the whole voltage range, than capacitors containing PEDOT-OMBs and PEDOT-OEBs. This is because PEDOT-OBs have a higher conductivity value, and therefore a lower ESR, than PEDOT-OMBs and PEDOT-OEBs. This also explains why PEDOT-OBs had a higher capacitance value than PEDOT-OMBs and PEDOT-OEBs. The doping level of PEDOT-OBs is higher than that of PEDOT-OMBs and PEDOT-OEBs; therefore, it have superior capacitance and lower ESR and leakage current values, because its dielectric surface area is much less damaged than that of PEDOT-OMBs and PEDOT-OEBs. The thermal degradation temperature of all polymerized materials is around 300–330 °C, indicating excellent thermal stability.

Acknowledgments

This work (Grants No. 00045311) was supported by Business for Cooperative R&D between Industry, Academy, and Research Institute funded Korea Small and Medium Business Administration in 2012.

References

[1] Y. Kudoh, S. Tsuchiya, T. Kojima, M. Fukuyama, S. Yoshimura, Synth. Met. 41 (1991) 1133–1136.

[2] F. Jonas, G. Heywang, Electrochim. Acta 39 (1994) 1345–1347.
[3] Y. Yasuo Kudoh, Toshikuni Kojima, Masao Fukuyama, Sohji Tsuchiya, Susumu Yoshimura, J. Power Sources 60 (1996) 157–163.
[4] S. Niwa, Y. Takemi, J. Power Sources 60 (1996) 165–172.
[5] Ming-Liao Tsai, Pei-Jiun Chen, Jing-Shan Do, J. Power Sources 133 (2004) 302–311.
[6] Hideo Yamamoto, Masashi Oshima, Tomio Hosaka, Isao Isa, Synth. Met. 104 (1999) 33–38.
[7] Yasuo Kudoh, Kenji Akami, Yasue Matsuya, Synth. Met. 102 (1999) 973–974.
[8] L. "Bert" Groenedaal, Friedrich Jonas, Dieter Freitag, Harald Pielartzik, John R. Reynolds, Adv. Mater. 12 (2000) 481–492.
[9] G. Zotti, S. Zecchin, G. Schiavon, F. Louwet, L. Groenendaal, X. Crispin, W. Osikowicz, W. Salaneck, M. Fahlman, Macromolecules 36 (2003) 3337–3344.
[10] L.A.A. Pettersson, T. Johansson, F. Carlsson, H. Arwin, O. Inganas, Synth. Met. 101 (1999) 198–199.
[11] Tae Young Kim, Chang Mo Park, Jong Eun Kim, Kwang S. Suh, Synth. Met. 149 (2005) 169–174.
[12] K. Katsunori Nogami, Kiyoshi Sakamoto, Teruaki Hayakawa, Masa-aki Kakimoto, J. Power Sources 166 (2007) 584–589.
[13] Hideo Yamamoto, Masashi Oshima, Minoru Fukuda, Isao Isa, Katsumi Yoshino, J. Power Sources 60 (1996) 173–177.
[14] Lampman Pavia, Vyvyan Kriz, Introduction to Spectroscopy, Brooks/Cole, Belmont, 2009.
[15] George Socrates, Infrared and Raman Characteristic Group Frequencies, John Wiley & Sons, New York, 2001.
[16] Tiejun Wang, Yingqun Qi, Jingkun Xu, Xiujie Hu, Ping Chen, Appl. Surf. Sci. 250 (2005) 188–194.
[17] John McMurry, Organic Chemistry, Thomson, Belmont, 2008.
[18] Chi-an Dai, Chun-jie Chang, Hung-yu Chi, Hung-ta Chien, Wei-fang Su, Wen-Yen Chiu, J. Polym. Sci. Part A: Polym. Chem. 46 (2008) 2536–2548.
[19] K.E. Aasmundtveit, E.J. Samuelsen, L.A.A. Pettersson, O. Inganas, T. Johansson, R. Feidenhans'l, Synth. Met. 101 (1999) 561–564.
[20] Yasuo Kudoh, Masao Fukuyama, Susumu Yoshimura, Synth. Met. 66 (1994) 157–164.
[21] Atsushi Nishino, J. Power Sources 60 (1996) 137–147.